IRSTI 533.9.01; 519.63; 519.684 10.26577/ijmph.202617110

A STUDY OF THE INFLUENCE OF THE HEIGHT OF NOISE PROTECTION BARRIERS ON THE DISPERSION OF POLLUTANTS IN A STREET CANYON BY THE METHOD OF COMPUTATIONAL FLUID DYNAMICS

A.A. Issakhov [1], **A. Shaken** [2], **A. Yamanov** [2], **A. Toibazarov** [2], **D. Mestoyeva** [2], **A. Lanskikh** [2], **A. Oshak** [2] and **Y. Namazaly** [2]

[1] *Kazakh-British Technical University, Almaty, Kazakhstan*

[2] *International school Haileybury, Almaty, Kazakhstan*

Email: alibek.issakhov@gmail.com

(Received 22 October 2025; revised 20 May 2026; accepted 30 May 2026)

Abstract. Urban air pollution poses a serious threat to public health, particularly in areas with heavy traffic, such as street canyons. This paper numerically investigates the effect of noise barriers of varying heights (0.1H, 0.2H, 0.3H, where H is the building height) on the dispersion of a passive pollutant (ethylene) in a street canyon model. The simulation is based on the Reynolds-averaged Navier-Stokes (RANS) equations and the SST k-ω turbulent model. The numerical model is verified by comparison with published experimental data and large eddy simulation (LES) results. Spatiotemporal distributions of pollutant concentrations are analyzed. The results show that a barrier of medium height (0.2H) forms a stable recirculation zone, acting as a "trap" for pollutants with maximum concentrations. A low barrier (0.1H) has a negligible effect, while a high barrier (0.3H) effectively screens the leeward zone but promotes pollutant accumulation on the windward side. A conclusion is drawn about the dual effect of barriers and the need to consider aerodynamic effects in their design.

Keywords: computational fluid dynamics (CFD), air pollution, street canyon, noise barrier, pollutant dispersion, RANS, SST k-ω.

INTRODUCTION

Air pollution in large cities remains one of the most pressing environmental issues. High traffic density and dense development create zones of elevated concentrations of harmful substances, posing a threat to public health. Motor vehicles are considered the primary source of pedestrian pollution, particularly in street canyons, where buildings restrict ventilation and contribute to the accumulation of emissions. Concentrations of nitrogen dioxide, carbon monoxide, and fine particles PM2.5 and PM10 in such areas often exceed health standards [1], [2]. Various approaches have been developed to analyze and predict the spread of pollutants in urban environments. Classic Gaussian models are simple and computationally inexpensive, but their application in complex urban environments is limited [3]. Computational fluid dynamics (CFD) methods provide more accurate results, taking into account street geometry, airflow patterns, and turbulent transport characteristics [4], [5]. Huertas and Prato [3] demonstrated that CFD modeling reproduces pollutant concentrations well near highways and demonstrates consistency with in-situ measurements. Zheng et al. [4] used a series of LES simulations to investigate pollutant dispersion in canyons of varying geometries and proposed recommendations for selecting the computational domain size to improve the reliability of the results. Baker et al. [5] applied LES to analyze the dispersion of reactive pollutants in street canyons and validated the approach with wind tunnel data. Particular attention is paid to the influence of structural elements of the urban environment. Reiminger et al. [6] examined the role of depressed road sections and demonstrated that the presence of depressions can significantly alter the pattern of pollutant concentrations in crosswinds. In another study, Reiminger et al. [7] proposed a method for taking into account the wind rose when estimating average annual concentrations and demonstrated the significance of climatic factors in CFD forecasts. In a study by Reiminger et al. [8], an analysis of the effectiveness of noise barriers was conducted, showing that their effect depends on wind speed and direction, as well as on atmospheric stratification. The influence of barriers has also been considered by other authors. Schulte et al. [9] showed that increasing the height of structures enhances the vertical dispersion of emissions, but does not always lead to a reduction in concentrations at the pedestrian level. Venkatram et al. [10] confirmed these findings based on in-situ measurements, noting up to a 40% reduction in pollutant levels near roads. A later study by Venkatram et al. [11] focused on the transport characteristics at the edges of barriers and showed that turbulent eddies at the boundary of the structure can lead to additional accumulation zones. The influence of street shape and building architecture is also being actively studied. Chang [12] used CFD to analyze point source dispersion between buildings and showed that street orientation relative to the wind plays a decisive role in the formation of high-concentration zones. Santiago et al. [13] demonstrated the importance of mesoscale wind conditions for the transport of PM10 particulate matter in urban areas. Baek et al. [14] showed that the density and location of green spaces can significantly alter the particle deposition pattern, and Qian et al. [15] noted that green walls and trees can significantly influence airflow patterns and canyon aerodynamics. Taken together, these studies indicate that CFD remains a key tool in analyzing dispersion processes in urban environments. However, modeling results are sensitive to the choice of turbulent model, mesh construction, and boundary conditions. Therefore, the development and verification of numerical approaches to urban aerodynamics problems remains highly relevant. This paper examines the impact of noise barriers of varying heights on pollutant dispersion processes in a street canyon. A numerical approach based on the Reynolds-averaged Navier-Stokes (RANS) equations, coupled with the SST k-ω turbulence model, is used for modeling. The focus is on analyzing the velocity and concentration fields of ethylene for various barrier configurations and comparing the obtained data with the results of existing numerical and experimental studies.

Materials and Methods

The simulation was based on the three-dimensional Navier-Stokes equations for an incompressible viscous gas, supplemented by a convection-diffusion equation for the pollutant. The flow was considered isothermal, with constant air and pollutant properties. To reduce computational costs, the model equations were Reynolds-averaged (RANS). In this case, turbulent stresses were approximated by the Boussinesq hypothesis, and the pollutant transport equation included an effective diffusion coefficient consisting of molecular and turbulent components.

$$\frac{\partial u_i}{\partial x_i} = 0$$

$$\frac{\partial(\rho u_i)}{\partial t} + \frac{\partial(\rho u_i u_j)}{\partial x_j} = -\frac{\partial p}{\partial x_i} +$$

$$\frac{\partial}{\partial x_j}\left[(\mu+\mu_t)\left(\frac{\partial u_i}{\partial x_j}+\frac{\partial u_j}{\partial x_i}\right)\right] - \frac{2}{3}\delta_{ij}\rho k$$

$$\frac{\partial \rho C}{\partial t} + \frac{\partial(\rho C u_i)}{\partial x_i} = \frac{\partial}{\partial x_i}\left[\rho\left(D+\frac{\nu_t}{Sc_t}\right)\frac{\partial C}{\partial x_i}\right]$$

where $\bar{u}_i$ is the average velocity vector, u_i' is the velocity vector fluctuation, $\bar{C}$ is the average concentration of the pollutant, C_i' is the concentration fluctuation, μ is the dynamic viscosity, $\overline{\rho(u_i'u_j')}$ is the Reynolds stress, $D_{eff} = D + \frac{\nu_t}{Sc_t}$ is the effective diffusion coefficient, including molecular diffusion D and turbulent kinematic viscosity ν_t, Sc_t is the turbulent Schmidt number, ρ is the air density, p is the pressure, and ν is the kinematic viscosity.

The SST k-ω model was chosen as the closing turbulent model. This choice was based on its versatility: it combines the advantages of the k-ε

model in developed flows and the k-ω model near walls. This allows it to accurately describe zones with high turbulent energy gradients and recirculation regions typical of street canyons and barriers.

$$\frac{\partial \rho k}{\partial t}+\frac{\partial(\rho k u_i)}{\partial x_j}=\frac{\partial}{\partial x_j}\left[\left(\mu+\frac{\mu_t}{\sigma_k}\right)\frac{\partial k}{\partial x_j}\right]+ P_k-\rho\beta^* k\omega$$

$$\frac{\partial \rho \omega}{\partial t}+\frac{\partial \rho\omega u_i}{\partial x_j}=\frac{\partial}{\partial x_j}\left[\left(\mu+\frac{\mu_t}{\sigma_\omega}\right)\frac{\partial \omega}{\partial x_j}\right]+ \frac{\alpha}{\nu_t}P_k-\rho\beta\omega^2+2(1-F_1)\rho\sigma_{\omega,2}\frac{1}{\omega}\frac{\partial k}{\partial x_j}\frac{\partial \omega}{\partial x_j}$$

Here, P_k is the turbulent energy source, μ_t is the turbulent viscosity, and F_1 is the mixing function. The model constants were used with their default values.

The finite volume method was used for numerical approximation. The pressure-velocity relationship was solved using the SIMPLE algorithm. A second-order approximation (upwind) was used for convective terms, and diffusion terms were approximated by central differences. The time step was set constant and selected based on the stability condition, and the calculation was continued until a statistically steady state was established.

Computational Domain Geometry and Boundary Conditions

A typical street canyon (Figure 1) formed by two parallel buildings was chosen as the study configuration. A linear pollutant source simulating vehicle emissions was located along the base of the canyon. Four scenarios were considered for the analysis: without a barrier and with barriers of heights 0.1H, 0.2H, and 0.3H, where H is the characteristic building height (H = 1.0 m). Airflow was specified transverse to the street, with a velocity of 1 m/s at the inlet boundary of the domain. Outflow conditions were used at the outlet. The upper boundary was modeled as a sliding wall condition (symmetry), and the lateral boundaries were also considered symmetrical. The surfaces of the buildings and barriers were assigned a no-slip condition. Ethylene (C_2H_4) with a density of $\rho = 1.137\,\mathrm{kg/m^3}$ and a dynamic viscosity of $\mu = 1.03\times10^{-5}\,\mathrm{kg/(m\cdot s)}$ was selected as the impurity. The impurity injection rate into the domain was 0.01923m/s. The indicated velocity corresponds to a volumetric flow rate of $Q_e =$ 3.0 l/min through a source cross-section and reproduces the experimental case [16]. The primary medium was air ($\rho = 1.225\mathrm{kg/m^3}$, $\mu = 1.79\times 10^{-5}\mathrm{kg/(m\ s)}$). The molecular diffusion coefficient for the mixture was $D = 2.88\times10^{-5}\mathrm{m^2/s}$.

Computational Mesh

To discretize the computational domain, a hybrid mesh was constructed, including tetrahe-

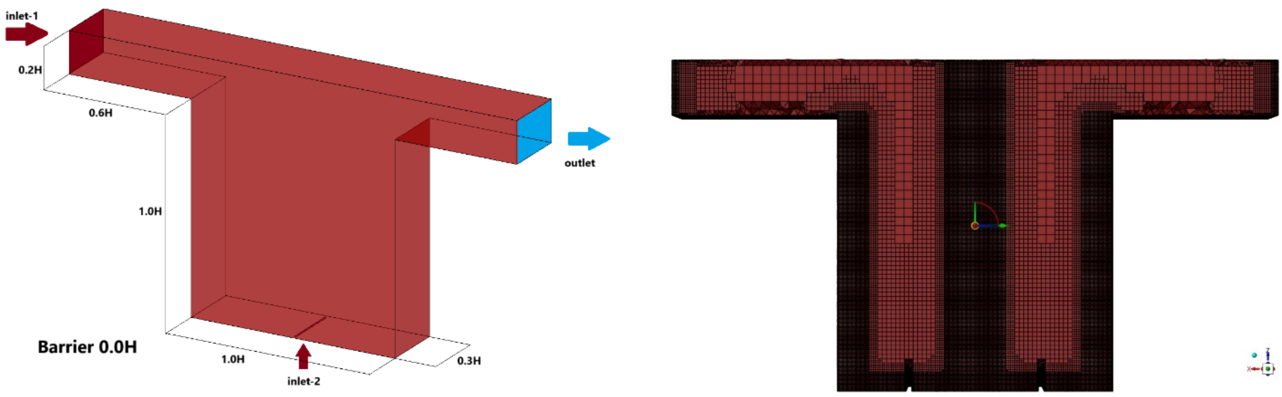

a) b)

Figure 1 - Computational domain configuration: a) schematic with main dimensions, b) computational grid.

Table 1 – Parameters of the computational grid for the main problem)

Mesh no.	Size min [m]	Size max [m]	Vol size [m]	Face size [m]	Elem. num.
1	0.25	0.5	0.5	0.1	369
2	0.125	0.25	0.25	0.05	863
3	0.03125	0.0625	0.0625	0.0125	8763
4	0.0078125	0.015625	0.015625	0.003125	227030
5	0.005	0.01	0.01	0.001	1195547

dral elements with localized densification near the source, walls, and barriers (Figure 1b). Prismatic layers were used at the boundaries to accurately describe boundary effects. A mesh convergence study was conducted. Five configurations with element numbers ranging from 3.7×10^2 to 1.2×10^6 were considered (Table 1). A comparison of the velocity and concentration profiles in the control sections showed that, starting with the third configuration, the differences become insignificant. The fifth mesh, with 1.2×10^6 elements, was used as the primary mesh, providing a balance between accuracy and cost.

Numerical Model Validation

To verify the validity of the chosen approach, a comparison was performed with experimental and numerical data presented in the work of Kikumoto and Ooka [16]. A barrier-free street canyon configuration was considered as a reference case. The geometry of the region, the physical properties of the gas, and the boundary conditions were fully consistent with the parameters used in this study. Kikumoto and Ooka [16] conducted both field experiments and large-eddy simulations (LES), allowing their results to be used as a baseline comparison criterion. The primary focus was on the velocity and concentration profiles of the pollutant at various control lines (Figure 2).

The obtained data showed that the use of the SST k- ω turbulent model provides good agreement with the experimental measurements. In some cross-sections, the concentration discrepancies did not exceed a few percent. Particularly close values were obtained near the windward side of the canyon, where flow dynamics are determined by large-scale eddy structures. To correctly resolve the near-wall flow at moderate y+ values, Spalding's wall law was applied. Thus, the chosen numerical scheme reproduces the characteristic features of pollutant transport and can be used for further analysis of the impact of barriers of varying heights.

Results and Analysis

Spatial Distribution of Concentrations. Analysis of the presented numerical modeling results (Figure 3) reveals characteristic patterns of ethylene propagation in a street canyon for various barrier configurations. All scenarios exhibit a common trend: by 200 seconds of simulation, the concentration distribution reaches a quasi-stationary state. In the early stages (t = 50 s), primary transport structures form, and by the final time step, the pollutant field stabilizes. For barrier-free configuration, a classic pattern of advective-diffusion transport is observed: ethylene propagates relatively freely through the canyon, forming a wide plume. Maximum values are recorded near the linear source, at the ground surface. By 200 seconds, the field stabilizes, with concentrations remaining highest near the leeward side of the street. For barrier height 0.1H, the low barrier causes only a weak disturbance of the flow. Immediately behind it, a localized recirculation zone is formed, where pollution accumulates on the windward side. However, overall, this configuration has a limited effect on the overall dispersion process. For barrier height 0.2H, the most pronounced effect is observed at the intermediate height. An intense circulation zone forms between the building and the barrier, acting as a

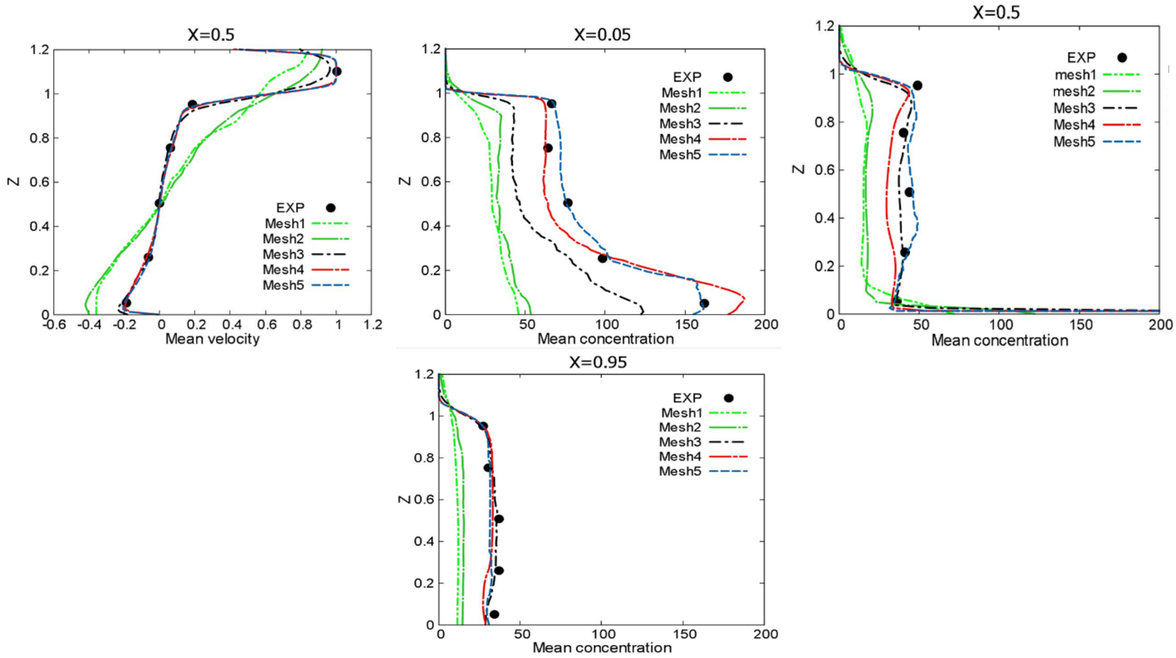

Figure 2 - Comparison of concentration for computational grids

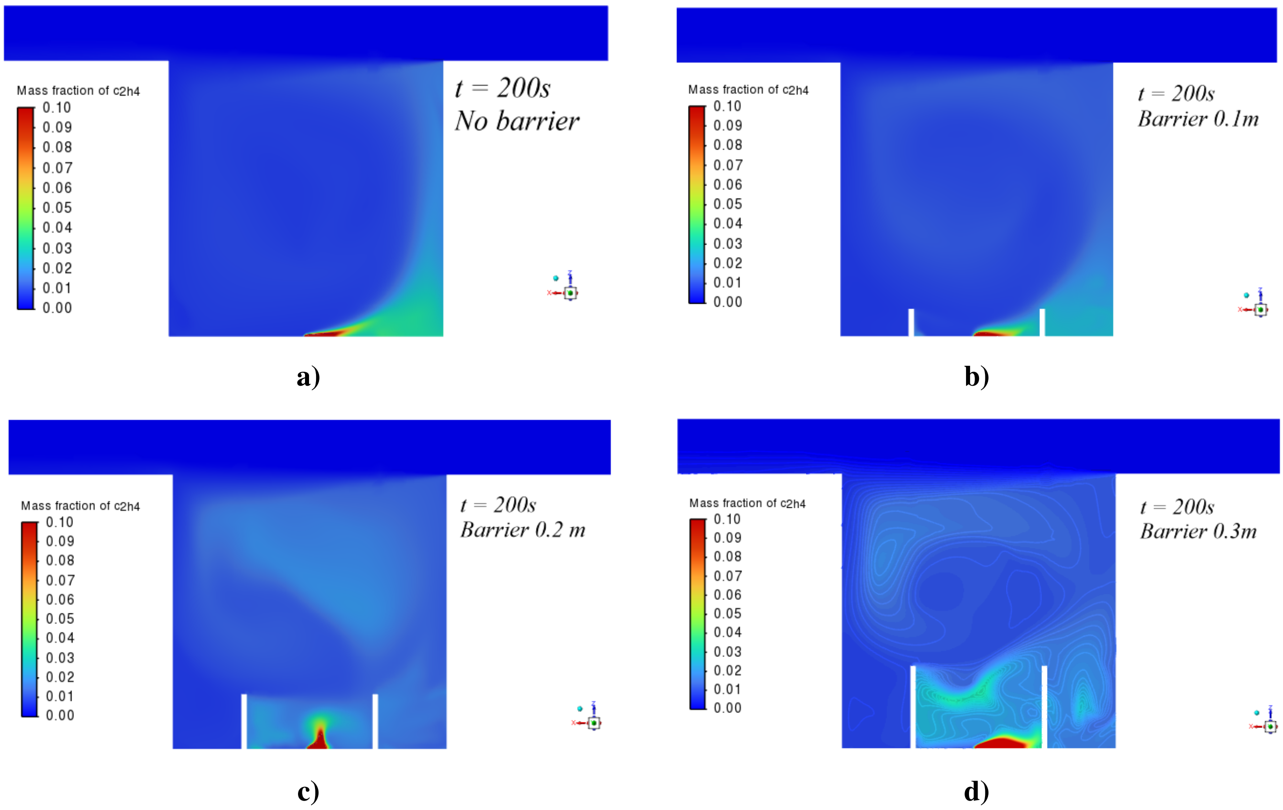

Figure 3 - Ethylene concentration distribution fields in a street canyon: a) without barrier, b) barrier of 0.1H height, c) barrier of 0.2H height, d) barrier of 0.3H height

"trap" for pollutants. Here, concentrations consistently reach maximum values (around 0.10 by mass fraction), while on the leeward side, a noticeable reduction in pollution levels is observed due to screening. For barrier height 0.3H, the greatest height demonstrates a dual effect. On the

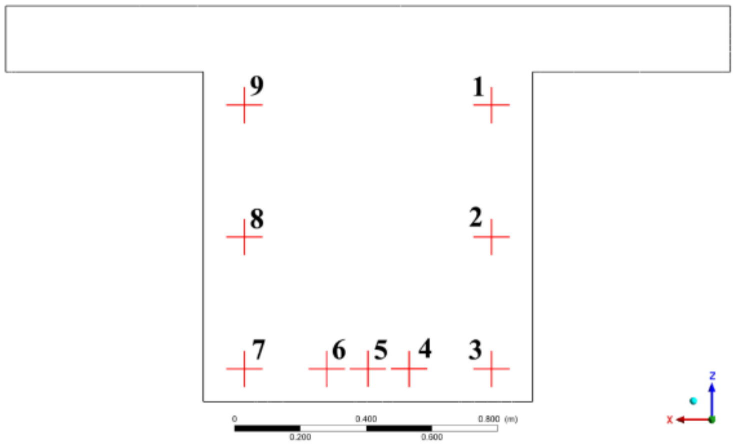

a)

b)

Figure 4 - Ethylene concentration value depending on time

one hand, the barrier effectively screens the leeward zone, virtually eliminating pollution penetration. On the other hand, the redistribution of flow over the structure leads to the formation of an extensive recirculation zone with moderate but consistently elevated concentrations. The mass fraction scale (0.00 - 0.10) allows for a comparative analysis of concentration levels. Maximum values (close to 0.10) are observed in the immediate vicinity of the source in the absence of a barrier and in the circulation zone in the 0.2H barrier configuration. The lowest background concentrations are recorded in shielded zones behind 0.2H and 0.3H barriers.

Temporal Changes in Concentration

Figure 4 shows the time series of concentrations at the monitoring points. The locations of the monitoring clocks are shown in Figure 4a. The largest fluctuations are recorded at points 1 and 3, located in the zone behind the barrier. For the 0.2H barrier, the fluctuation amplitude is maximum, which is associated with the formation of unstable vortex structures and recirculation. At point 9, located closer to the leeward side of the canyon, the concentrations are lower, indicating a decrease in pollutant influx into this area. A comparison of the scenarios shows that low barriers (0.1H) have little effect on pollutant distribution. Medium barrier heights (0.2H) create conditions for enhanced pollutant accumulation due to the formation of stable recirculation zones. High barriers (0.3H) reduce pollutant influx into the leeward side of the street but simultaneously help retain it between the building and the barrier.

Conclusion

This study conducted a numerical study of ethylene propagation in a street canyon with various noise barrier configurations. A RANS approach with the SST k-ω turbulence model was used for modeling, allowing us to reproduce the dynamics of pollutant dispersion processes in complex urban geometries. Analysis of the concentration distribution showed that:

- in the absence of a barrier, the pollutant spreads relatively freely along the canyon, forming a stable plume with maximum values on the downwind side;
- a low barrier height (0.1H) has only a localized effect, creating a small recirculation zone behind the structure but without changing the overall transport pattern;
- at a medium barrier height (0.2H), a distinct closed circulation zone forms, acting as a "trap" for the pollutant. The highest concentrations are recorded here, while a significant decrease in pollutant levels is observed in the downwind zone;
- A high barrier (0.3H) provides the strongest shielding of the leeward side of the canyon; however, flow redistribution leads to the formation of a large area of moderate but consistently elevated concentrations behind the structure. Thus, barrier height has a dual effect: it can significantly reduce concentrations in the leeward zones, but simultaneously contribute to the accumulation of pollutants in the immediate vicinity of the source.

The obtained results highlight the need for an integrated approach in the design of noise protection structures, considering not only acoustic efficiency but also their impact on aerodynamics and air quality in the urban environment.

Author Contributions: Conceptualization, A.I.; methodology, A.Issakhov; software, A. Issakhov, A. Shaken, A. Yamanov, A. Toibazarov, D. Mestoyeva, A. Lanskikh, A. Oshak, Y. Namazaly; validation, A. Issakhov, A. Shaken, A. Yamanov, A. Toibazarov, D. Mestoyeva, A. Lanskikh, A. Oshak, Y. Namazaly; formal analysis, A. Issakhov, A. Shaken, A. Yamanov, A. Toibazarov, D. Mestoyeva, A. Lanskikh, A. Oshak, Y. Namazaly; investigation, A. Issakhov; resources, A.Issakhov; data curation, A.Issakhov; writingoriginal draft preparation, A. Issakhov; writingreview and editing, A. Issakhov; visualization, A.Issakhov; supervision, A.Issakhov; All authors have read and agreed to the published version of the manuscript.

References

[1] World Health Organization, “Ambient (outdoor) air pollution.” 2022. https://www.who.int/en/news-room/fact-sheets/detail/ambient-(outdoor)-air-quality-and-health Accessed: 2025-09-06.

[2] Xia, F., X. Cheng, Z. Lei, J. Xu, Y. Liu, Y. Zhang, and Q. Zhang. “Heterogeneous impacts of local traffic congestion on local air pollution within a city: Utilizing taxi trajectory data.” *Journal of*

Environmental Economics and Management 122 (2023): 102896. https://doi.org/10.1016/j.jeem.2023.102896

[3] Huertas, J. I. and D. F. Prato. "Cfd modeling of near-roadway air pollution." *Environmental Modeling & Assessment* 25, no. 2 (2020): 129–145. https://doi.org/10.1007/s10666-019-09666-w

[4] Zheng, X., H. Montazeri, and B. Blocken. "Large-eddy simulation of pollutant dispersion in generic urban street canyons: Guidelines for domain size." *Journal of Wind Engineering and Industrial Aerodynamics* 211 (2021): 104527. https://doi.org/10.1016/j.jweia.2021.104527

[5] Baker, J., H. L. Walker, and X. Cai. "A study of the dispersion and transport of reactive pollutants in and above street canyonsa large eddy simulation." *Atmospheric Environment* 38, no. 39 (2004): 6883–6892. https://doi.org/10.1016/j.atmosenv.2004.08.051

[6] Reiminger, N., X. Jurado, L. Maurer, J. Vazquez, and C. Wemmert. "Influence of depressed road configuration on downwind pollutant concentrations: A cfd study under various thermal stability conditions." *Journal of Wind Engineering and Industrial Aerodynamics* 235 (2023): 105361. https://doi.org/10.1016/j.jweia.2023.105361

[7] Reiminger, N., X. Jurado, J. Vazquez, C. Wemmert, N. Blond, J. Wertel, and M. Dufresne. "Methodologies to assess mean annual air pollution concentration combining numerical results and wind roses." *Sustainable Cities and Society* 59 (2020): 102221. https://www.sciencedirect.com/science/article/pii/S2210670720302080

[8] Reiminger, N., X. Jurado, J. Vazquez, C. Wemmert, N. Blond, M. Dufresne, and J. Wertel. "Effects of wind speed and atmospheric stability on the air pollution reduction rate induced by noise barriers." *Journal of Wind Engineering and Industrial Aerodynamics* 200 (2020): 104160. https://doi.org/10.1016/j.jweia.2020.104160

[9] Schulte, N., M. Snyder, V. Isakov, D. Heist, and A. Venkatram. "Effects of solid barriers on dispersion of roadway emissions." *Atmospheric Environment* 97 (2014): 286–295. https://doi.org/10.1016/j.atmosenv.2014.08.026

[10] Venkatram, A., V. Isakov, P. Deshmukh, and R. Baldauf. "Modeling the impact of solid noise barriers on near road air quality." *Atmospheric Environment* 141 (2016): 462–469. https://doi.org/10.1016/j.atmosenv.2016.07.005

[11] Venkatram, A., D. K. Heist, S. G. Perry, and L. Brouwer. "Dispersion at the edges of near road noise barriers." *Atmospheric Pollution Research* 12, no. 2 (2021): 367–374. https://doi.org/10.1016/j.apr.2020.11.017

[12] Chang, C.-H. "Computational fluid dynamics simulation of concentration distributions from a point source in the urban street canyons." *Journal of Aerospace Engineering* 19, no. 2 (2006): 80–86. https://doi.org/10.1061/(ASCE)0893-1321(2006)19:2(80)

[13] Santiago, J., B. Sanchez, C. Quaassdorff, D. de la Paz, A. Martilli, F. Martín, R. Borge, E. Rivas, F. Gómez-Moreno, E. Díaz, B. Artiñano, C. Yagüe, and S. Vardoulakis. "Performance evaluation of a multiscale modelling system applied to particulate matter dispersion in a real traffic hot spot in madrid (spain)." *Atmospheric Pollution Research* 11, no. 1 (2020): 141–155. https://doi.org/10.1016/j.apr.2019.10.001

[14] Baek, S., J. Kim, and J. Kang. "Impact of green infrastructure on pm10 in port-adjacent residential complexes: A finite volume method-based computational fluid dynamics study." *Sustainable Cities and Society* 115 (2024): 105815. https://doi.org/10.1016/j.scs.2024.105815

[15] Qian, X., X. Zhang, A. Weerasuriya, and J. Zhai. "Designing green walls to mitigate fine particulate pollution in an idealized urban environment." *Sustainable Cities and Society* 113 (2024): 105640. https://doi.org/10.1016/j.scs.2024.105640

[16] Kikumoto, H. and R. Ooka. "Large-eddy simulation of pollutant dispersion in a cavity at fine grid resolutions." *Building and Environment* 127 (2018): 127–137. https://doi.org/10.1016/j.buildenv.2017.11.005

Information about authors

Alibek Issakhov *– PhD, Professor, School of Applied Mathematics, Kazakh-British Technical University (Almaty, Kazakhstan, email: Alibek.issakhov@gmail.com);*
Amira Shaken *– student, Haileybury International School, Almaty, Kazakhstan.*
Artur Yamanov *– student, Haileybury International School, Almaty, Kazakhstan.*
Aldiyar Toibazarov *– student, Haileybury International School, Almaty, Kazakhstan.*
Dalia Mestoyeva *– student, Haileybury International School, Almaty, Kazakhstan.*
Angelina Lanskikh *– student, Haileybury International School, Almaty, Kazakhstan.*

Arnur Oshak *– student, Haileybury International School, Almaty, Kazakhstan.*
Erdulat Namazaly *– student, Haileybury International School, Almaty, Kazakhstan.*